Supplementary text

Introduction

The conceptual distance between internal medicine terminology and classification ("functional somatic syndromes", FSS) and the category of "somatoform disorders" in the psychiatric classification system prevented the integration of both frameworks, as most somatoform disorder diagnoses, unlike FSS, required the presence of *multiple* "medically unexplained somatic symptoms" (MUS) and/or an established role of psychological factors [1-3]. Recently, both conceptual frameworks have come closer together, as exemplified by the new DSM-V category/diagnosis of "somatic symptom disorder" (SSD). SSD criteria abandoned the requirement for multiple MUS, shifting emphasis to a positive diagnosis based on a) "one or more somatic symptoms that are distressing or result in significant disruption of daily life", b) "excessive thoughts, feelings, behaviors related to the somatic symptoms or associated health concerns" and c) persistence [1, 4]. It is likely that the SSD concept will capture an (important) subgroup of the FSS/FGID cases [1], especially in tertiary care, although data are currently lacking. In parallel, there is a tendency within the "Rome IV" committees who are currently revising FGID diagnostic criteria, to incorporate psychosocial factors into their classification system (unpublished).

Methods

Radiotracer characteristics and preparation

Brain CB_1 receptor imaging was performed using the radiotracer [^{18}F]MK-9470, which is an inverse agonist with high affinity and specificity for the human CB_1 receptor [5]. The precursor of [^{18}F]MK-9470, obtained from Merck Research Laboratories (MRL, West Point, PA, USA), was labeled on-site with 2-[^{18}F]fluoroethylbromide.[5] The final product was obtained after high pressure liquid chromatography (HPLC) separation and had a radiochemical purity >

95%. Specific activity was higher than 100 GBq/µmol. The tracer was administered in a sterile solution of 5 mM sodium acetate buffer with pH 5.5 containing 6% ethanol.

Imaging procedure

All subjects fasted for at least four hours prior to their PET session. To minimize head movement during the PET acquisition, each subject was positioned with the head placed in a vacuum cushion and the body was fixed before the dynamic PET emission scan. Each subject received the radiotracer in a slow bolus injection, under standardized injection circumstances. The mean injected [^{18}F]MK-9470 dose was 275.3±45.4 MBq (range: 224.1 - 331.1 MBq) for FD1, 326.5±44.3 MBq (range: 231.2 - 374.2 MBq) for FD2, and 324.1±50.8 MBq (range: 167.3 - 357.2 MBq) for HC (none of the pairwise differences significant).

PET acquisitions were performed using an ECAT EXACT HR+ scanner (Siemens, Erlangen, Germany) in three-dimensional mode. A 30 minute dynamic PET scanning session, divided into six 5-minute frames, was started 90 min after radioligand injection [6-8]. PET images were reconstructed with a standard three-dimensional filtered backprojection algorithm including scatter and attenuation correction (^{68}Ge source). The resulting transverse and axial spatial resolution was approximately 4 mm.

Additionally, to exclude any structural brain abnormalities and to anatomically co-register with the PET images, all subjects underwent a standard structural magnetic resonance imaging (MRI) scan on a 1.5 Tesla scanner (Siemens Sonata or; Philips Medical Systems Achieva or Intera or Gyroscan NT), using a 3-dimensional T1-weighted Magnetization Prepared Rapid Acquisition Gradient Echo (3D-MPRAGE) sequence. The following acquisition parameters were used: repetition time, 10 milliseconds; echo time, 4 milliseconds; flip angle, 8°; voxel size: 1x1x1 mm.

Image processing

CB_1 receptor availability was quantified using the modified standard uptake value (mSUV), a validated non-invasive simplified quantification method [5-12] mSUV images were generated

by summation of the activity concentration between 90 to 120 minutes post-injection, corrected for tracer injected dose and subject's body weight: mSUV = ([activity concentration (kBq/mL) x (subject's weight [kg] + 70)/2] / injected dose (MBq)) [13].

Parametric maps of CB_1 receptor availability were generated by means of PMOD v 3.0 (PMOD Technologies, Zürich, Switzerland). For each subject, PET frames were realigned and co-registered to the individual magnetic resonance imaging (MRI) scan using SPM8 (Statistical Parametric Mapping, Wellcome Department of Imaging Neuroscience, London, UK). The co-registered [^{18}F]MK-9470 mSUV images were then spatially normalized to a specific CB_1 receptor template constructed in Montreal Neurological Institute (MNI) space (voxel size 2 x 2 x 2 mm) [11], masked within the brain 80% isocontour of the CB_1 receptor template and finally smoothed with a Gaussian kernel (full-width-at-half maximum 10 mm) in SPM8.

Based on previous literature on FD and the role of the ECS in both (visceral) nociception and the homeostatic and hedonic regulation of food intake [14, 15], twenty-three a priori defined regions of interest (ROI) were taken from an in-house previously created set of ROI defined on the CB_1 receptor template [11] representing cortical Brodmann areas (BA) and subcortical grey matter structures. As the CB_1 receptor template did not include ROI for PAG and medulla, an additional ROI analysis for these brain regions was performed in SPM8 ($p_{FWE-corr}<.05$ at voxel level). The PAG region of interest was defined as the union of two spheres (6mm radius) with the center at the Montreal Neurological Institute (MNI) coordinates [x = 6, y = -32, z = -12] and [x = -6, y = -32, z = -12].[16]. The medulla region of interest was defined using the TD Lobes atlas, available in the WFU-Pickatlas toolbox in SPM8.[17, 18] The subdivision proposed by Vogt *et al* was used for the cingulate cortex.[19] The full list of the predefined ROI is shown in *Supplementary Table 1*. Additionally, subcortical brain areas were individually adjusted by delineating these regions manually on transverse slices of T1 images, as described previously [10].

For visualization purposes the PET results were superimposed on a normalized canonical image namely the ch2better template available in MRIcron software.

Results

Participant characteristics at inclusion

Four out of 12 patients (33%) met the diagnostic criteria for co-morbid IBS [20]; the average PHQ-15 score was 13.3±5.6 (range 6-24), indicating high levels of "somatization", further confirmed by the fact that 8/12 (75%) and 5/12 (42%) of the patients scored higher than the cutoff for "medium" (>10) and "high" (>15) somatic symptom severity [21]. Based on these results, it is likely that the majority of the patients fulfill the DSM-IV criteria for "undifferentiated somatoform disorder" (full-blown DSM-IV "somatization disorder" was excluded based on the MINI). Z-scores on the 4 PCCL subscales were within the same range as the norm population of chronic (back) pain patients [22]: catastrophizing (-1.09±.38), pain coping (-0.66±..87), internal pain control (0.56±1.04) and external pain control (-0.50±.28). The total IAS score was 34.0±10.76, which is considerably higher than scores reported in general population samples, ranging from 20-23 [23, 24]. Further, the score is comparable to a large MUS patient sample with and without DSM-IV somatoform disorder diagnosis (excluding hypochondriasis) (35.9±13.5 and 32.9±14.4, respectively) [25], as well as to a major depression sample without personality disorder (32.4±16.6) [26], but lower than a sample with a DSM-IV hypochondriasis diagnosis (51.7±15.0) [25]. When looking at the a priori defined IAS subscales [27], mainly scores on the "health habits" (7.7±2.0), "treatment experience" (6.4±2.7) and "effect of symptoms" (5.3±2.8) subscales are high. The latter two subscales have been shown to load on an "illness behaviour" construct (healthcare seeking, interference with daily activities) in factor analytical studies [27]. The scores for the "illness behaviour" subscales found in our study are in line with findings in general psychiatric and somatoform patients samples (including hypochondriasis patients who typically don't score higher than other somatoform patients on "illness behaviour") [23, 25, 28, 29] and higher than

general population samples [23, 30, 31]. The other seven subscales, including "health habits", load on a second "health anxiety" factor, which has been shown to discriminate between hypochondriasis patients and others [27]. The scores for these "health anxiety" subscales found in our study are similar to general psychiatric samples [24, 26], similar to or somewhat lower than somatoform patient samples without hypochondriasis [25, 28] and clearly lower compared to hypochondriasis samples [23-25, 28].

Taken together, these results indicate that our FD patients are generally characterized by a) "one or more somatic symptoms (as evident from FD diagnosis, FD symptom questionnaire & PHQ-15 scores) that are distressing or result in significant disruption of daily life" (as evident from IAS "illness behaviour" scores), b) "excessive thoughts, feelings, behaviours related to the somatic symptoms or associated health concerns" (as evident from PCCL scores at the level of chronic pain patients & IAS scores at the level of somatoform disorder patients), without being primarily being characterized by hypochondriasis or health anxiety (as evident from IAS "health anxiety" scores that are clearly lower compared to hypochondriasis samples) and c) persistent symptoms (median duration of FD symptoms 18.5 [12.75-45] months). Thus, even though diagnostic criteria for SSD were not available at the time of recruitment, it is likely that the majority of our patient sample would fulfill DSM-V diagnostic criteria for SSD (and not Illness Anxiety Disorder).

Evolution of 9 individual dyspepsia symptoms

The severity ratings of 9 individual dyspeptic symptoms at both scan sessions are listed in *Supplementary Table 2* and visualized in *Supplementary Figure 1,* showing a decrease in ratings for all individual symptoms. Significant differences were found for discomfort and postprandial fullness (P=.009 and .035, respectively) and the differences for epigastric pain and belching were borderline significant (both P= .051). The lack of full significance for some of the symptoms may be due to the small sample size, as large effect sizes (Cohen's $d > 0.8$) were found for the decrease in discomfort, postprandial fullness and early satiety ratings. Medium effect sizes ($0.5 <$ Cohen's $d < 0.8$) were observed for the decrease in ratings of

epigastric pain, nausea and belching. The effect size for the differences in ratings of bloating, epigastric burning and vomiting was small (Cohen's $d < 0.5$).

Supplementary Tables

Region of interest	Brodmann area	lateralization
Amygdala		left & right
Insula		left & right
Caudate nucleus		left & right
Putamen		left & right
Nucleus accumbens		left & right
Hypothalamus		midline
Periaqueductal gray[A]		midline
Medulla[B]		midline
Posterior midcingulate cortex / Posterior cingulate cortex	BA 23	midline
Subgenual anterior cingulate cortex	BA 25	midline
Perigenual anterior cingulate cortex / Anterior midcingulate cortex	BA 24 & 32	midline
Ventrolateral prefrontal cortex	BA 47	left & right
Dorsolateral prefrontal cortex	BA 9 & 46	left & right
Ventromedial prefrontal cortex	BA 10 & 11	left & right
Secondary somatosensory cortex	BA 43	left & right

Supplementary table 1: A priori regions of interest used in the study

Except for the periaqueductal gray and medulla regions, all regions of interest were taken from a previously created set of regions of interest defined on the CB_1 receptor template representing cortical Brodmann areas and subcortical grey matter structures [11]. The corresponding Brodmann areas are indicated when applicable.

[A]The periaqueductal gray region of interest was defined as the union of two spheres (6mm radius) with the center at MNI coordinates 6, -32, -12 and -6, -32, -12. The MNI coordinates were taken from Vincent et al [16].

[B]The medulla region of interest was defined using the Labels atlas, available in the WFU Pickatlas toolbox in SPM8 [17, 18].

Dyspeptic symptoms	**FD1 > FD2 (%)**	**$P_{uncorrected}$**	**Cohen's *d***
Discomfort	*-0.30 ± 0.26*	*0.009*	*1.38*
Epigastric pain	-0.19 ± 0.24	0.051	0.71
Postprandial fullness	*-0.15 ± 0.18*	*0.035*	*0.97*
Bloating	-0.04 ± 0.31	0.73	0.16
Early satiety	-0.22 ± 0.33	0.081	0.96
Nausea	-0.15 ± 0.34	0.23	0.50
Vomiting	-0.07 ± 0.28	0.45	0.33
Epigastric burning	-0.04 ± 0.42	0.80	0.10
Belching	-0.19 ± 0.24	0.051	0.74

Supplementary Table 2: Severity of nine dyspeptic symptoms at the first and second PET scan

Functional dyspepsia patients scored the intensity of nine dyspeptic symptoms over the preceding 3 months at the first and second PET scan (FD1 and FD2, respectively), on a Likert scale from 0 to 3. The effect sizes are reflected by Cohen's *d* (0.2 = small effect; 0.5 = medium effect; > 0.8: large effect). Data represented as mean ± SD. italic = significant at $P_{uncorrected}<.05$

Regions of interest	FD1 > HC (%)	$P_{bootstrap\text{-}corrected}$	Cohen's *d*
Amygdala	*19.80 ± 22.60*	*.020*	*1.23*
Insula	*25.00 ± 22.64*	*.007*	*1.46*
Caudate nucleus	*27.72 ± 23.23*	*.003*	*1.49*
Putamen	*22.78 ± 22.30*	*.014*	*1.28*
Nucleus accumbens	*21.10 ± 22.77*	*.026*	*1.15*
Hypothalamus	*21.43 ± 21.84*	*.016*	*1.27*
Posterior midcingulate cortex / Posterior cingulate cortex	*19.90 ± 21.05*	*.022*	*1.17*
Subgenual anterior cingulate cortex	*23.44 ± 21.89*	*.009*	*1.35*
Perigenual anterior cingulate cortex / Anterior midcingulate cortex	*25.66 ±21.89*	*.005*	*1.46*
Ventrolateral prefrontal cortex	*20.59 ± 21.11*	*.020*	*1.18*
Dorsolateral prefrontal cortex	*19.64 ± 22.24*	*.033*	*1.10*
Ventromedial prefrontal cortex	*20.55 ± 21.28*	*.019*	*1.22*
Secondary somatosensory cortex	*19.19 ± 22.21*	*.038*	*1.07*

Supplementary Table 3: Regional cerebral cannabinoid-1 receptor availability in functional dyspepsia patients versus healthy controls: results of region of interest analysis

In a priori regions of interest, mean modified standard uptake values (mSUVs) were calculated and compared using unpaired Student's *t*-tests. Bootstrapping was used to correct for multiple testing. Data are represented as mean ± SD. The effect sizes are reflected by Cohen's *d* (0.2 = small effect; 0.5 = medium effect; > 0.8: large effect). FD1: first PET scan session in functional dyspepsia patients; HC: healthy controls, italic = significant at $P_{bootstrap\text{-}corrected}<.05$

Regions of interest	FD2 > FD1 (%)	$P_{uncorrected}$
Amygdala	-1.39 ± 12.11	.58
Insula	-3.25 ± 11.95	.47
Caudate nucleus	-2.06 ± 13.35	.48
Putamen	-3.10 ± 11.88	.42
Nucleus accumbens	-2.20 ± 13.10	.46
Hypothalamus	0.46 ± 13.45	.73
Posterior midcingulate cortex / Posterior cingulate cortex	-3.12 ± 11.25	.42
Subgenual anterior cingulate cortex	-1.34 ± 14.22	.58
Perigenual anterior cingulate cortex / Anterior midcingulate cortex	-1.37 ± 13.36	.58
Ventrolateral prefrontal cortex	-2.83 ± 11.96	.48
Dorsolateral prefrontal cortex	-2.06 ± 11.82	.57
Ventromedial prefrontal cortex	-2.06 ± 12.51	.53
Secondary somatosensory cortex	-1.83 ± 12.04	.55

Supplementary Table 4: Regional cerebral cannabinoid-1 receptor availability in functional dyspepsia patients at the first PET scan and after an average follow-up period of 36 months: results of region of interest analysis

In a priori regions of interest, mean modified standard uptake values (mSUVs) were calculated and compared using paired Student's *t*-tests. Data represented as mean ± SD. FD1: first PET scan session; FD2: second PET scan session.

Supplementary Figures

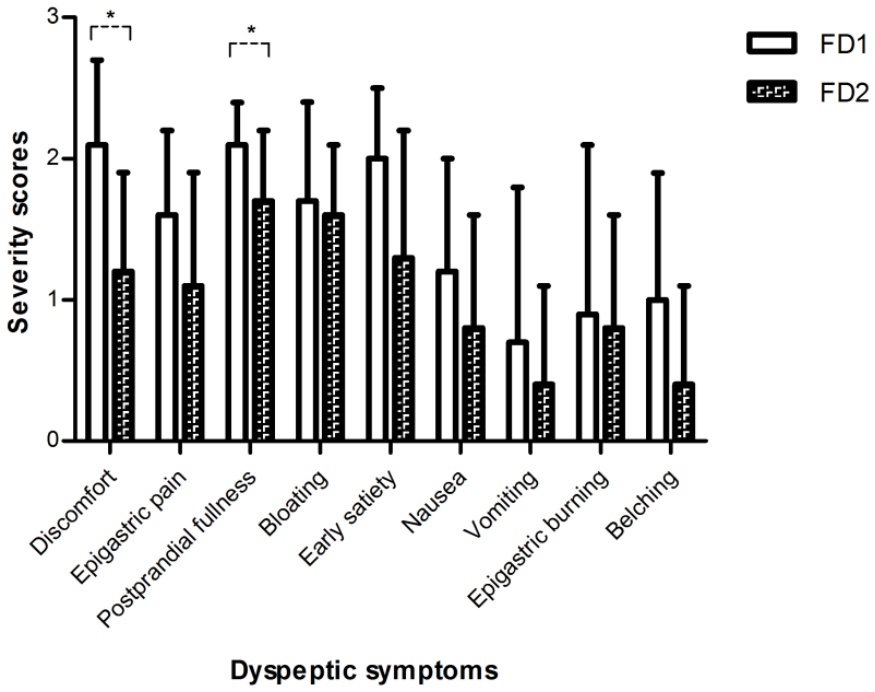

Supplementary Figure 1: Severity ratings of nine dyspeptic symptoms by functional dyspepsia patients, at the first PET scan (FD1) and after an average follow-up of 36 months (FD2)

Despite the clearly declining trend in all symptoms, only discomfort and postprandial fullness reached significance level of $P_{uncorrected}<.05$. However, epigastric pain and belching are also (borderline) significant. Large effect sizes of the differences in ratings between the two PET scans were observed in discomfort, postprandial fullness and early satiety. In nausea, epigastric pain and belching medium effect of differences in severity ratings were found. Although, the effect sizes are substantial, the (relatively) small sample probably precludes some ratings differences to reach significance. Data represented as mean±SD. * = significant $P_{uncorrected}<.05$

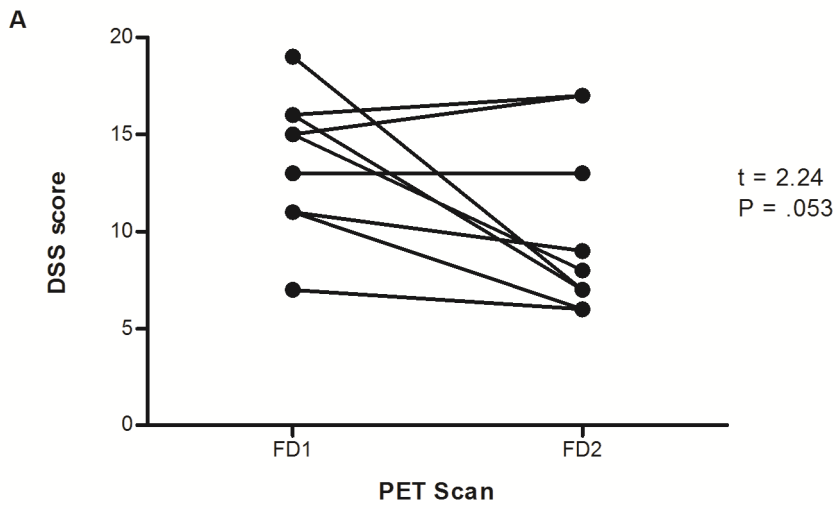

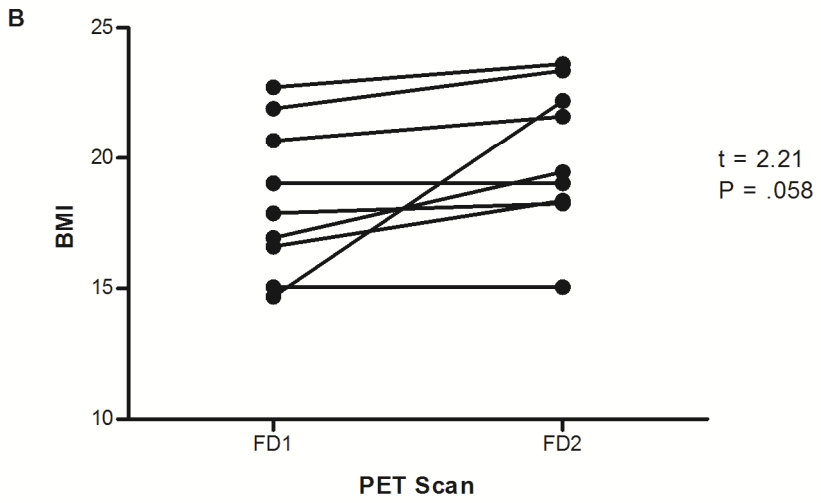

Supplementary Figure 2: Evolution in dyspepsia symptoms and body mass index in functional dyspepsia patients after an average follow-up of 36 months

A. *Dyspepsia Symptom Severity (DSS):* Compared to the first PET scan session (FD1), most patients reported improved dyspepsia symptoms at the second PET scan (FD2).

Only two of the nine patients rated their symptoms more severe at the moment of the second scan. The effect of difference in severity ratings between the two PET scans is large (Cohen's *d* = 0.89). To compare the DSS scores a paired Student's *t*-test was performed.

B. *Body Mass Index (BMI):* Seven out of nine patients gained weight between the two PET scan sessions. To compare the BMI paired. The effect of difference in weight between the two PET scans is medium (Cohen's *d* = 0.60). Student's *t*-test with P<.05 was performed.

Supplementary references

1 Dimsdale JE, Creed F, Escobar J, Sharpe M, Wulsin L, Barsky A, Lee S, Irwin MR, Levenson J: Somatic symptom disorder: An important change in dsm. J Psychosom Res 2014;75:223-228.

2 Henningsen P, Herzog W: Irritable bowel syndrome and somatoform disorders. J Psychosom Res 2008;64:625-629.

3 American Psychiatric Association: Diagnostic and statistical manual of mental disorders, ed 4. Washington, DC, American Psychiatric Association, 1994.

4 American Psychiatric Association: Diagnostic and statistical manual of mental disorders, ed 5. Arlington, VA, American Psychiatric Publishing, 2013.

5 Burns HD, Van Laere K, Sanabria-Bohórquez S, Hamill TG, Bormans G, Eng WS, Gibson R, Ryan C, Connolly B, Patel S, Krause S, Vanko A, Van Hecken A, Dupont P, De Lepeleire I, Rothenberg P, Stoch SA, Cote J, Hagmann WK, Jewell JP, Lin LS, Liu P, Goulet MT, Gottesdiener K, Wagner JA, de Hoon J, Mortelmans L, Fong TM, Hargreaves RJ: [18f]mk-9470, a positron emission tomography (pet) tracer for in vivo human pet brain imaging of the cannabinoid-1 receptor. Proc Natl Acad Sci U S A 2007;104:9800-9805.

6 Gerard N, Pieters G, Goffin K, Bormans G, Van Laere K: Brain type 1 cannabinoid receptor availability in patients with anorexia and bulimia nervosa. Biol Psychiatry 2011;70:777-784.

7 Van Laere K, Casteels C, Dhollander I, Goffin K, Grachev I, Bormans G, Vandenberghe W: Widespread decrease of type 1 cannabinoid receptor availability in huntington disease in vivo. J Nucl Med 2010;51:1413-1417.

8 Van Laere K, Casteels C, Lunskens S, Goffin K, Grachev ID, Bormans G, Vandenberghe W: Regional changes in type 1 cannabinoid receptor availability in parkinson's disease in vivo. Neurobiol Aging 2012;33:620.e621-628.

9 Sanabria-Bohórquez SM, Hamill TG, Goffin K, De Lepeleire I, Bormans G, Burns HD, Van Laere K: Kinetic analysis of the cannabinoid-1 receptor pet tracer [(18)f]mk-9470 in human brain. Eur J Nucl Med Mol Imaging 2010;37:920-933.

10 Ceccarini J, De Hert M, Van Winkel R, Peuskens J, Bormans G, Kranaster L, Enning F, Koethe D, Leweke FM, Van Laere K: Increased ventral striatal cb1 receptor binding is related to negative symptoms in drug-free patients with schizophrenia. Neuroimage 2013;79:304-312.

11 Van Laere K, Goffin K, Casteels C, Dupont P, Mortelmans L, de Hoon J, Bormans G: Gender-dependent increases with healthy aging of the human cerebral cannabinoid-type 1 receptor binding using [(18)f]mk-9470 pet. Neuroimage 2008;39:1533-1541.

12 Van Laere K, Goffin K, Bormans G, Casteels C, Mortelmans L, de Hoon J, Grachev I, Vandenbulcke M, Pieters G: Relationship of type 1 cannabinoid receptor availability in the human brain to novelty-seeking temperament. Arch Gen Psychiatry 2009;66:196-204.

13 Thie JA, Hubner KF, Isidoro FP, Smith GT: A weight index for the standardized uptake value in 2-deoxy-2-[f-18]fluoro-d-glucose-positron emission tomography. Mol Imaging Biol 2007;9:91-98.

14 Bermudez-Silva FJ, Cardinal P, Cota D: The role of the endocannabinoid system in the neuroendocrine regulation of energy balance. J Psychopharmacol 2012;26:114-124.

15 Di Marzo V, Ligresti A, Cristino L: The endocannabinoid system as a link between homoeostatic and hedonic pathways involved in energy balance regulation. Int J Obes 2009;33 Suppl 2:S18-24.

16 Vincent K, Warnaby C, Stagg CJ, Moore J, Kennedy S, Tracey I: Brain imaging reveals that engagement of descending inhibitory pain pathways in healthy women in a low endogenous estradiol state varies with testosterone. Pain 2013;154:515-524.

17 Maldjian JA, Laurienti PJ, Kraft RA, Burdette JH: An automated method for neuroanatomic and cytoarchitectonic atlas-based interrogation of fmri data sets. Neuroimage 2003;19:1233-1239.

18 Maldjian JA, Laurienti PJ, Burdette JH: Precentral gyrus discrepancy in electronic versions of the talairach atlas. Neuroimage 2004;21:450-455.

19 Vogt BA: Pain and emotion interactions in subregions of the cingulate gyrus. Nat Rev Neurosci 2005;6:533-544.
20 Longstreth GF, Thompson WG, Chey WD, Houghton LA, Mearin F, Spiller RC: Functional bowel disorders. Gastroenterology 2006;130:1480-1491.
21 Kroenke K, Spitzer RL, Williams JBW: The phq-15: Validity of a new measure for evaluating the severity of somatic symptoms. Psychosom Med 2002;64:258-266.
22 de Gier M, Vlaeyen JWS, Van Breukelen G, Stomp SGM, ter Kuile M, Kole-Snijders AMJ, Spinhoven P: Pijn coping en cognitie lijst. Validering en normgegevens. Maastricht, Pijnkenniscentrum Maastricht, 2004.
23 Noyes Jr R, Happel RL, Yagla SJ: Correlates of hypochondriasis in a nonclinical population. Psychosomatics 1999;40:461-469.
24 Kellner R, Abbott P, Winslow WW, Pathak D: Fears, beliefs, and attitudes in dsm-iii hypochondriasis. J Nerv Ment Dis 1987;175:20-25.
25 Hiller W, Rief W, Fichter MM: Dimensional and categorical approaches to hypochondriasis. Psychol Med 2002;32:707-718.
26 Demopulos C, Fava M, McLean NE, Alpert JE, Nierenberg AA, Rosenbaum JF: Hypochondriacal concerns in depressed outpatients. Psychosom Med 1996;58:314-320.
27 Sirri L, Grandi S, Fava GA: The illness attitude scales. Psychother Psychosom 2008;77:337-350.
28 Pauli P, Alpers GW: Memory bias in patients with hypochondriasis and somatoform pain disorder. J Psychosom Res 2002;52:45-53.
29 McBeth J, Macfarlane GJ, Hunt IM, Silman AJ: Risk factors for persistent chronic widespread pain: A community-based study. Rheumatology 2001;40:95-101.
30 McBeth J, Macfarlane GJ, Benjamin S, Silman AJ: Features of somatization predict the onset of chronic widespread pain: Results of a large population-based study. Arthritis Rheum 2001;44:940-946.
31 Speckens AEM, Spinhoven P, Sloekers PPA, Bolk JH, van Hemert AM: A validation study of the whitely index, the illness attitude scales, and the somatosensory amplification scale in general medical and general practice patients. J Psychosom Res 1996;40:95-104.